# SAFETY CASE REPORT

# ADDENDUM

# Doel 3

## Reactor Pressure Vessel Assessment

26 April 2013
v.u. Electrabel nv, Simón Bolívarlaan 34, 1000 Brussel

Electrabel
GDF SUEZ

# Contents



Electrabel
GDF SUEZ

# 1 Executive Summary

In 2012, indications were found inside the shells of the Doel 3 and Tihange 2 reactor pressure vessels (RPVs). A series of analyses, tests, and inspections have shown that these indications are hydrogen flakes that do not affect the structural integrity of either RPV, regardless of the operating mode, transient, or accident condition. An independent review team consisting of national and international experts and academics confirmed this outcome.

The results of the investigations were synthesized in comprehensive Safety Case Reports, and submitted to the Federal Agency for Nuclear Control (FANC) in December 2012.

On 30 January 2013, the FANC provided Electrabel with a Provisional Evaluation Report emphasizing that the licensee has performed a profound piece of work, that the information was given in all transparency, and that the reports are of excellent quality. The FANC stated that it saw no elements that would have led to a permanent shutdown of the nuclear power plants. Nevertheless, the FANC asked for additional information before making a recommendation on a potential restart. This was summarized as a set of requirements in the Provisional Evaluation Report. In response, Electrabel submitted an Action Plan on 4 February 2013, which was discussed with the authorities. It was approved by the FANC on 7 February 2013 and started immediately.

The present document gives a structured and complete answer to each of the FANC's requirements for the Doel 3 RPV. It also provides the results and conclusions of additional analyses, tests, and inspections that were performed to complement the Safety Case.

The results of these complementary tests and analyses lead to the following conclusions:

- UT inspection technique is valid
- Hydrogen flaking is confirmed, understood, and stable
- Affected material is sound and with good properties
- Structural integrity is demonstrated with significant safety margins
- Load test did not reveal any unexpected condition nor induced any flaw evolution

Based on all of these additional tests, analyses, and inspections, Electrabel is convinced that the structural integrity of the Doel 3 RPV has been demonstrated and that all safety requirements are met. Therefore, Electrabel asks for the immediate restart of the Doel 3 nuclear power plant.

Electrabel
GDF SUEZ

# 1.1 Context of the Addendum

The Doel 3 and Tihange 2 RPV Safety Cases submitted in December 2012 were evaluated by the FANC together with Bel V, AIB Vinçotte, and national and international expert groups. During the assessment process, the experts were able to discuss their questions with the Electrabel Project Team, which, in turn, provided complementary information and answers.

On 30 January 2013, the FANC provided Electrabel with a Provisional Evaluation Report stating that there is no element that would have led to a permanent shutdown of the units. However, some open issues remain to be addressed before the reactors can be restarted. In response to the Provisional Evaluation Report, Electrabel submitted an Action Plan, which addresses the safety concerns at the origin of the FANC's requirements and that need to be addressed before restart.

The present document complements the Safety Case for the Doel 3 RPV. It summarizes the answers to the requirements stipulated by the FANC and the conclusions of additional analyses, tests, and inspections conducted since December 2012.

# 1.2 Action Plan

The actions can be grouped into five topics:

- Ultrasonic (UT) inspections
- Origin and evolution of the indications
- Material properties
- Structural integrity assessment
- Load tests and subsequent UT inspections

Electrabel has executed the actions required by the FANC. The results of these actions are discussed in the following chapters:


**Figure 1.1: Overview of actions**

# 1.3 Conclusions

Based on the additional tests, analyses, and inspections that were performed to complement the 2012 Safety Case, the following conclusions can be made.

## UT inspection technique is valid

Further investigation—including extensive destructive tests on the VB395/1 reference block—confirm that the applied UT inspection technique (straight beam) is valid and appropriate for sizing the quasi-laminar indications found in the Doel 3 RPV. More specifically, the technique correctly detects and sizes all of the found indications, including the partially hidden and higher tilted ones. Additional analyses have also revealed a good correlation between the tilts evaluated by the straight beam UT technique and those investigated by the phased array technique. Moreover, no correlation was found between the 45° T UT responses and any radial or volumetric component of the flake.

During the 2012 UT inspection, precise and complete data for each individual flaw's position and dimensions were collected. This addendum offers an overview of statistics to ensure a good understanding of the flaw distribution.

Periodic in-service inspections corroborate that the cladding is sound.

In addition, no critical hydrogen flakes are to be expected in the areas of the RPV's inner surface where the geometry affects the UT technique's capability.

## Hydrogen flaking is confirmed, understood, and stable

Not all forged components of the Doel 3 RPV contain the same amount of hydrogen flakes. They also have different ingot sizes and combined sulphur and hydrogen contents. Analysis of these characteristics reveals a good correlation with the amount of flakes found in each forged component.

Additional investigations on the VB395 reference block confirm that the hydrogen flakes were initiated during manufacturing in macro-segregated areas, in particular in ghost lines at manganese sulphide inclusions. There is no detectable difference in residual hydrogen content measured in specimens with or without flakes. Residual content is confirmed to be very low.

Tests also corroborate that the hydrogen flaking in the VB395 material is representative for the hydrogen flaking in the Doel 3 RPV on various characteristics.

The stable character of the hydrogen flakes was already confirmed in the initial Safety Case Report.

## Affected material is sound and with good properties

Complementary tests performed on the Doel 3 H1 nozzle cut-out material show that the ghost lines have no significant effect on the Charpy impact test results or fracture toughness properties.

Additional tests on the VB395 material containing hydrogen flakes confirm the limited effect of hydrogen flaking on the material properties. The ductility of the material in the ligaments between flakes is similar to the ductility of the material free of flakes. Large-scale tests on material containing flakes confirm the good ductility and load bearing capacity. The fracture toughness of the ligaments between flakes is only slightly lower as compared to the flake-free material. This is confirmed through tests on specimens with a flake as crack tip.

Since it is demonstrated that the flaking observed in the VB395 material is representative for the flaking in the reactor pressure vessels, the findings and conclusions of the tests performed on the VB395 material can be transferred to the Doel 3 RPV. As a consequence, the $RT_{NDT}$ shift of 50 °C considered in the Structural Integrity Analyses is confirmed to be conservative.

### Structural integrity is demonstrated with significant safety margins

The calculations confirm that the acceptance criteria of the deterministic studies are met with a very significant safety margin:

- A complementary elasto-plastic analysis for the most penalizing flaw configuration shows that the ASME III Primary Stress limits are respected.
- Only eleven flaws or groups of flaws in the Doel 3 RPV exceed the flaw-screening criterion, but still meet the acceptability criterion. Additional refined analyses show substantial margins.

Additional sensitivity analyses reveal a significant safety margin for the structural integrity assessment. Even in the case where the most penalizing flaw would be located at the clad-base metal interface with a 5° larger inclination, a significant margin remains. Moreover, the integration of potentially unreported flaws does not affect the structural integrity.

The suitability and conservativeness of the Structural Integrity Assessment is fully demonstrated through large-scale tensile and bending validation tests on material containing flakes.

### Load test did not reveal any unexpected condition nor induced any flaw evolution

The Doel 3 RPV was subjected to a load test with acoustic emission (AE) measurements and subsequent UT inspection. The AE measurements performed did not reveal any source or area for which complementary investigations are required. The flaw indications reported by the UT inspection are fully consistent with the findings of the 2012 RPV inspection. In addition, all examination results confirm that the load test did not modify the condition of the material.

## 1.4 Independent Review

As with the 2012 Safety Case Reports, the Service de Contrôle Physique (SCP) of Electrabel again conducted an independent analysis of the project deliverables as well as of the present document. The SCP Review Team will issue its independent advice in an addendum to the previous advice report supplied in December 2012.

# 2 Ultrasonic Inspection

## 2.1 Inspection Results

### 2.1.1 Flaw Distribution Statistics

During the 2012 UT inspection, precise and complete data about each individual flaw's position and dimensions were collected. In order to provide a good understanding of the flaw distribution, the data have been processed in different ways.

#### Requirement

During the discussion of the Safety Case Report, the need for a better understanding of how the flaws are distributed in the RPV shells was expressed.

#### Steps taken

Each and every flaw detected by the 2012 UT inspection in the Doel 3 RPV is known in terms of its exact position in the RPV wall and its maximum dimensions in three orthogonal directions. This enables the calculation of different flaw statistics, such as:

- **Flaw density**

  The average flaw density in the first 100 mm of the Doel 3 lower core shell is 2.1 flaws/litre. The maximum is 25.8 flaws/litre.

- **Distance between a flaw and its closest neighbour**

  The average distance between the flaws in the Doel 3 RPV shells is 20.4 mm. The maximum distance is 565 mm.

- **Potential correlations with the fluence distribution**

  It was demonstrated that there is no correlation between the positions of the indications and the fluence distribution. Likewise, the Safety Case Report had already concluded that there is no correlation between indication size and fluence distribution.

- **Trends between the flaws' inclinations and the flaws' positions**

  No trend was found between the flaws' inclinations and their vertical or angular position in the RPV wall.

## 2.1.2 Cladding and Internal Surface of Forgings

The cladding was not taken into consideration in the Structural Integrity Assessment (SIA), in conformance with the ASME code. Periodic in-service inspections confirm that the cladding is sound.

### Cladding

During the discussion of the Safety Case Report, it was asked whether or not the cladding affects the Safety Case and whether or not it is sound.

In accordance with the ASME code, the cladding is not taken into consideration in the SIA of the RPVs. Therefore, the Safety Case does not rely on the condition of the cladding.

The clad layer was subjected to manufacturing examination, as well as in-service inspection. Qualified visual testing is conducted during each ten-year interval on the entire inner surface of the RPV. These inspections confirm that the cladding is sound.

### Internal surface of forgings

During the discussion of the Safety Case Report, a question was asked about the results of the surface inspections performed after final machining, and before cladding.

RDM performed Magnetic Testing (MT) on all Doel 3 RPV components. Cockerill repeated the MT on the inner surface of all parts before austenitic clad deposit. All examination reports have been retrieved in the manufacturing files, but no flaw detection was reported on any occasion. MT can only detect flaws oriented perpendicularly to the induced magnetic flux lines, i.e. flaws perpendicular to the examination surface. Clearly, laminar flaws would not produce MT indications.

## 2.1.3 Non-Inspectable Areas

The capability of the UT inspection technique is to some extent affected by the geometrical features of specific areas of the RPV inner surface. The Doel 3 RPV has four of these areas on its inner surface. Near three of these areas, no clusters of flaws are detected. Therefore, no hydrogen flakes are expected there. In the fourth area—behind the brackets—the presence of flakes cannot be excluded. However, the brackets would protect potentially hidden flakes in terms of stress and toughness. Hence, such potentially hidden flakes are not considered to be critical.

### Requirement

In 'Doel 3 and Tihange 2 reactor pressure vessels – Provisional evaluation report (30 January 2013)', the FANC requires the following with regard to non-inspectable areas:

> *The licensee shall demonstrate that no critical hydrogen flake type defects are expected in the non-inspectable areas.*

### Steps taken: investigation into four locations

The geometry of the RPV is different from the circular, cylindrical form that it has elsewhere at four locations on its inner surface. This affects the capability of the UT inspection technique to detect flaws in those areas.

The locations are as follows:

- In the RPV flange: a diameter step and a tapered transition between two areas with different internal diameters.
- In the nozzle shell: a tapered transition.
- Welded on the inner surface of the lower core shell: four guiding brackets for the RPV internals.

In the Doel 3 RPV, brackets could potentially hide hydrogen flakes. However, these brackets protect such potential flaws in terms of stress and toughness. The other three locations are far from the clusters of flaws. Hence, it can be concluded that no critical hydrogen flake-type defects are expected in the non-inspectable areas of the Doel 3 RPV.

## 2.1.4 Potentially Unreported Higher Tilted Flaws

Additional examinations of higher tilted flaws confirm that the 2012 straight beam UT inspections correctly detected and sized all hydrogen flakes in the block VB395/1. Flaws with an inclination up to 20°, that would potentially not have been reported, have been determined as a function of the position in the RPV wall. These potential flaws are considered in the Sensitivity Analyses.

### Requirement

In 'Doel 3 and Tihange 2 reactor pressure vessels – Provisional evaluation report (30 January 2013)', the FANC requires the following with regard to tilted flaws:

> *The licensee shall demonstrate that the applied ultrasonic testing procedure allows the detection of the higher tilt defects in the Doel 3/Tihange 2 data (2012 inspections) with a high level of confidence.*

### Step 1: Additional examinations of higher tilted flaws

The initial step taken in response to this requirement was to revisit the block VB395/1 UT results in search of hydrogen flakes with the highest tilts available.

**EAR** is one of the three UT transducers on the MIS-B machine that inspects the first 30 mm of the RPV shells.

The ultrasonic examination—as part of the UT validation on block VB395/1—uncovered approximately 370 flaws. Eight flaws or 2% of the approximately 370 flaws were higher tilted, meaning inclined between 10° and a maximum of 15° along the X or Y-axis. Five of these eight flaws were cut, two of which had already been investigated during the UT validation (see Safety Case Report, Chapter 4.3.4 UT Validation). The results from these five investigations confirm that these flaws were correctly detected and sized by the straight beam UT inspection technique.

## Step 2: Experimental evaluation of the inspection sensitivity

The 2012 UT inspections of the two RPVs were executed with a very high sensitivity level, which enhances the detection and reporting of higher tilted indications. By their nature, higher tilted indications are less reflective than laminar indications.

The same inspection sensitivity applied to the VB395/1 block, shows that all indications are adequately detected, sized, and reported using the reporting threshold applied during the 2012 RPV inspection.

## Step 3: UT sensitivity study as input for the structural integrity assessment

The CIVA modelling software (developed by the Commissariat à l'Energie Atomique et aux Energies Alternatives—CEA) allows the simulation of UT responses from virtual flaws. By varying their dimension, inclination, and depth, it enables the determination of hypothetical RPV flaws that would have generated UT response amplitudes below the reporting levels applied during the 2012 UT inspections at Doel 3 and Tihange 2.

A range of inclinations up to 20° has been investigated, which is well beyond the 15° maximum inclination (see Step 1).

For the first 25 mm in the RPV wall, covered by the EAR (see previous page) transducer, the analysis was carried out with a reporting threshold value of -18 dB. Therefore, no additional potentially unreported flaws need to be considered.

For the depth range between 25 and 120 mm, Figure 2.1 shows the size of the largest flaw with the conservative 20° inclination that would potentially not have been reported, as a function of the position in the RPV wall. The impact that these potentially unreported flaws could have on the results of the Structural Integrity Assessment (SIA) is addressed as part of the Sensitivity Analyses in Chapter 5.

**Shell VB395** is a forged shell that was manufactured by AREVA as part of a steam generator for a 1300 MW-type power plant. It was rejected during manufacturing in 2012 due to the presence of a large number of hydrogen flakes.

Shell VB395 is made out of steel type 18MND5. Its chemical composition is in accordance with the specifications of steel type SA-508 Class 3 used for the Doel 3 and Tihange 2 RPVs. Also, its dimensions are comparable to the dimensions of the RPV shells.

An elaborate testing program was performed on blocks extracted from this shell, both with and without hydrogen flakes.

The following reference blocks are mentioned in the Safety Case and the Addendum:

**Block VB395/1:** taken from the lower part of the shell, contains hydrogen flakes, and was used for UT validation

**Blocks VB395/51 to VB395/54:** taken from the upper part of the shell and free of hydrogen flakes

**Blocks VB395/61 and VB395/62:** taken from the lower part of the shell and contains hydrogen flakes

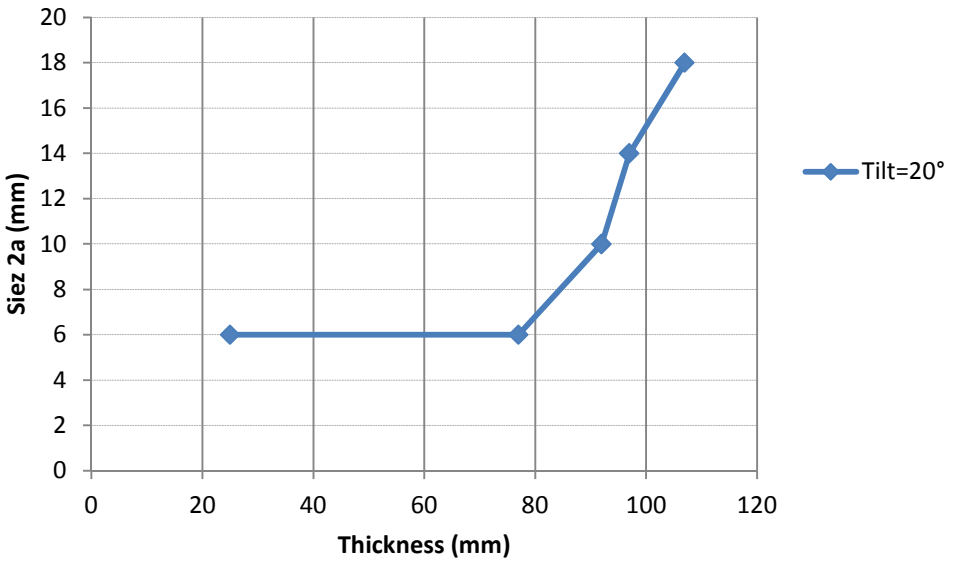


**Figure 2.1: Size of the largest flaws with 20° inclination potentially not reported by UT inspection**

## Conclusions

The UT validation (see Safety Case Report, Chapter 4.3.4 UT Validation) on block VB395/1 had already led to the conclusion that all hydrogen flakes in VB395/1, both the tilted and higher tilted, were correctly detected and sized using the UT procedure (straight beam) applied on site. Additional examinations on higher tilted flaws confirm that the 2012 straight beam UT inspections correctly detected and sized all hydrogen flakes in VB395/1.

Flaws with an inclination up to 20°—that would potentially not have been reported—have been determined as a function of the position in the RPV wall. These potential flaws are considered in the Structural Integrity Assessment as part of the Sensitivity Analyses (see Chapter 5).

# 2.2 Ultrasonic Testing Validation (UT Validation)

## 2.2.1 Indications with a 45° T Shear Wave Response

During the 2012 in-service inspection of the reactor pressure vessels (RPVs), a number of very weak 45° T shear wave UT responses were observed. The macro-graphical examination of three samples of block VB395/1 showed that there is no correlation between the 45° T UT responses and any radial or volumetric component of the flake.

### Requirement

In 'Doel 3 and Tihange 2 reactor pressure vessels – Provisional evaluation report (30 January 2013)', the FANC requires the following with regard to 45° T reflections:

> *The licensee shall present the detailed report of all macrographical examinations including the sample with the 45°T reflections and shall also analyse and report additional samples with 45°T reflectivity.*

### Steps taken: three samples examined

During the 2012 in-service inspection of the RPVs, a number of 45° T UT responses were observed at very low amplitudes. The current action investigated the actual nature of the 45° T UT responses, since no such response is expected from nearly laminar hydrogen flakes.

A total of three samples from block VB395/1 showing 45° T UT responses were investigated and reported. The samples were chosen based on the amplitude of their 45° T response and on the spatial match between the straight beam and the 45° T response on the given flaw.

- **First sample:** a detailed report was provided, with pictures, of all earlier macro-graphical examinations on block VB395/1, including the examination of a 45° T reflection sample.

  The Authorized Inspection Agency (AIA) recommended using block VB395/1 to determine the actual nature of the 45° T UT responses.

- **Two additional samples:** two samples with 45° T reflectivity were analyzed by macro-graphical examination in the context of this action.

### Conclusions

The macro-graphical examination of the three samples taken from block VB395/1 confirmed that there is no correlation between the 45° T UT responses and any radial or volumetric component of the flake.

## 2.2.2 Partially Hidden Indications

Two samples with multiple hydrogen flakes were taken from block VB395/1 and examined. The dimensions resulting from their ultrasonic examination were compared to the results of their destructive examination. The comparison confirms the capability of straight beam ultrasonic testing (UT) to correctly detect and size hydrogen flakes that are partially hidden by others.

### Requirement

In 'Doel 3 and Tihange 2 reactor pressure vessels – Provisional evaluation report (30 January 2013)', the FANC requires the following with regard to partially hidden flaws:

> *The licensee shall include a set of defects partially hidden by other defects for macrographical examination, to confirm whether the sizing method continues to function well.*

### Steps taken: destructive examination of two samples

A first sample taken from block VB395/1 showed a partially hidden flake. This sample contains two partially overlapping indications: the lower one is partially hidden by the upper one. The destructive examination of this sample confirms the correct sizing of the flaws by straight beam UT inspection.

Also from block VB395/1, a second sample was extracted from a zone with a very high density of indications. A destructive examination was performed and reported. This sample contained four partially overlapping flakes, all correctly detected and sized by UT.

The destructive examination of both samples confirms that the straight beam UT examination applied during the 2012 in-service inspection ensures a good detection and sizing of indications. Moreover, the UT dimensions were oversized on both the X and Y axes.

## 2.2.3 Inclination of Flaws Detected by Ultrasonic Testing

During the 2012 in-service inspection, ultrasonic testing (UT) was performed using a straight ultrasonic beam. The results contained a number of indications with tilts that were evaluated from the straight beam information. At the UT validation, the tilts of the indications in block VB395/1 were determined using a phased array inspection.

The tilts of the flaws in the block VB395/1 were re-evaluated using the same straight beam UT method as applied on site. The results confirm a very good correlation between both methods.

### Requirement

In 'Doel 3 and Tihange 2 reactor pressure vessels – Provisional evaluation report (30 January 2013)', the FANC requires the following with regard to the measurement of flaw tilts identified by ultrasonic examination (UT) in block VB395/1:

> *The licensee shall re-analyse the tilts of the defects in the block VB395/1 with the same method as applied on-site.*

### Steps taken

During the 2012 in-service inspection, the UT examinations were performed using a straight ultrasonic beam. The results contained a number of indications with tilts.

At the UT validation, the tilts of the indications in block VB395/1 were determined using a phased array inspection, which led to the following conclusions:

- The range of inclinations found in block VB395/1 is similar to the range found on site during the UT inspections.
- The typical inclinations found in block VB395/1 are similar to the typical inclinations found on site during the UT inspections.

A re-analysis of the flaw inclinations in block VB395/1 was conducted using the straight beam UT method, as applied on site.

Estimating a flaw's angle using straight beam UT was carried out on a sample of indications. The angle was calculated from the difference between time of flight to both end points of the UT signal, and on its length measured by UT.

The investigation shows a very good correlation in the results between both methods.

# 3 Origin and Evolution of the Indications

## 3.1 Root Cause: Link between Manufacturing and Flake Occurrence

Not all forged components of the Doel 3 and Tihange 2 reactor pressure vessels (RPVs) contain the same amount of hydrogen flakes. Based on an analysis of the ingot size and the combined sulphur and hydrogen content, the forgings were ranked according to their susceptibility to hydrogen flaking. This revealed a good correlation with the amount of flakes found in each forged component.

### Requirement

During the discussion of the Safety Case Report, it was noted that the root cause analysis did not explain why the hydrogen-induced degradation did not evenly affect all the forged components of the Doel 3 and Tihange 2 RPVs, though their hydrogen content is comparable.

### Steps taken

As explained in the Safety Case Report, there is a consensus in current literature that three factors are necessary for the creation of hydrogen flakes (see Figure 3.1). Each factor is in turn influenced by several parameters.

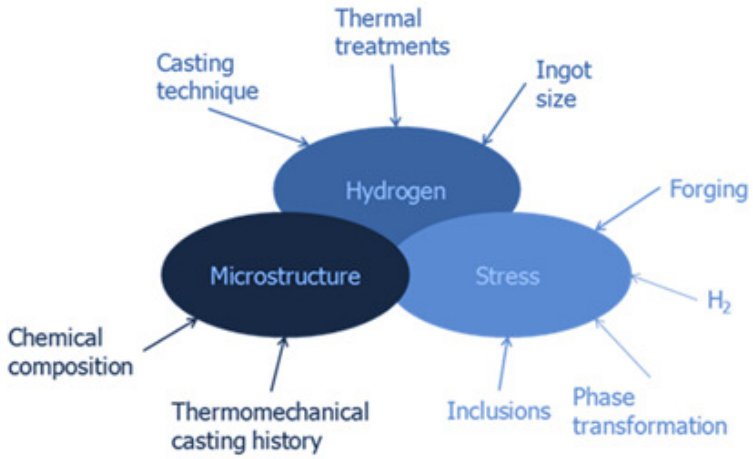


**Figure 3.1: Factors contributing to the creation of hydrogen flakes**

Casting, forging, and heat treatment are similar for the Doel 3 and Tihange 2 RPVs. A comparison between the forgings can be made based on the few parameters that are different from one component to another, such as ingot size and hydrogen and sulphur contents.

For these parameters, Electrabel has analyzed the susceptibility to hydrogen flaking of the forged components, based on the following:

- Literature shows that the risk of hydrogen flaking increases with the ingot size. Therefore, the largest ingots (110 ton ingots for the core and nozzle shells) are considered to be twice as susceptible to hydrogen flaking as the smallest ingot (55 ton ingot for the Tihange 2 transition ring).
- The forging's susceptibility to hydrogen flaking as a function of its hydrogen and sulphur content is assessed based on the graph in Fruehan's paper 'A Review of Hydrogen Flaking and Its Prevention'.

The analysis enables the ranking of the Doel 3 and Tihange 2 forgings according to their susceptibility to hydrogen flaking in three categories: forgings with low susceptibility, forgings with medium susceptibility where very limited flaking might be present, and forgings with high susceptibility.

### Conclusion

The results of the analysis show a good correlation between susceptibility levels and actual presence of flakes: the most affected forgings indeed fall in the high susceptibility category.

# 3.2 Phenomenology of Hydrogen Flaking

As mentioned in the Safety Case Report, literature shows that the indications in the RPV shell could be associated with a zone of macro-segregations that originate from the fabrication process. This was confirmed by new tests on reference block VB395/1.

Moreover, the flaws are situated in very specific locations: the so-called 'ghost lines', which correspond to the residual features of the ingot after forging. In addition, the representativeness of the reference block VB395/1 and the flaking mechanism have been confirmed. Bridging was found to occur only between flakes that are very close to each other, under circumstances that exclusively exist during manufacturing.

### Additional analysis

In the Safety Case Report, the flaking mechanism, its influencing factors, and root cause analysis were described on the basis of literature. Additional investigations were conducted to confirm this.

### Steps taken

Tests have been performed on a significant number of specimens from block VB395/1, which contains hydrogen flakes. The following aspects were investigated on hundreds of samples:

- Flake position, sizing, inclination, and morphology.
- Situation of flakes in relation to macro-segregations, micro-structural characteristics, including hardness.
- Micro-fractographic examination of twenty open flakes.
- Localized chemical analysis.

For the VB395/62 block, the carbon segregation profile has been compared to the distribution of flakes through the thickness, showing a one-to-one correspondence, as shown below. This confirms that the flaking occurs in macro-segregated areas.

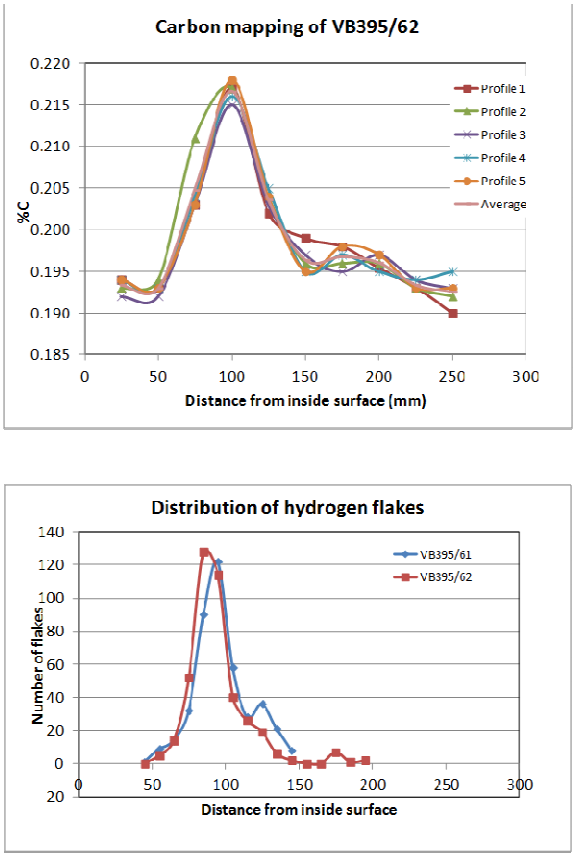


**Figure 3.2, top: Carbon mapping, bottom: Distribution of indications in function of the position in depth**

## Conclusions

The investigations confirm the **flaking mechanism**. The flaking occurs in macro-segregated areas. The hydrogen flakes initiated in ghost lines at manganese sulphides, during manufacturing, due to the local simultaneous presence of:

- A high quantity of hydrogen (zones of last solidification and last transformation of austenite to ferrite).
- Stresses (e.g. forging deformation stresses, phase transformation stresses).
- A sensitive structure resulting from high segregation (martensite).

The micro-fractographic examination shows that the material between two flakes, which have been identified separately using non-destructive testing, is sound. **Bridging** can only occur between flakes that are very close to each other, under circumstances that exclusively exist during manufacturing.

The above conclusions are fully in line with what is described in the literature.

**Ghost lines** (*veines sombres* in French) are quasi-axial alignments of localized macro-segregated areas enriched in alloying elements and impurities. They correspond to the residual features after forging of segregates formed during the ingot solidification. These areas are flattened and fragmented during forging. Typical dimensions are 30 mm x 16 mm with a thickness of 0.5 to 1.5 mm. They are easily recognizable since they appear as dark zones after etching. Ghost lines are commonly found in all types of forgings.

# 3.3 Residual Hydrogen

Additional tests confirm that there is no significant amount of residual hydrogen present inside the metal, nor in the flakes. Therefore, the material properties are unaffected.

## Requirement

In 'Doel 3 and Tihange 2 reactor pressure vessels – Provisional evaluation report (30 January 2013)', the FANC requires the following with regard to potential residual hydrogen:

> *The licensee shall perform additional measurements of the current residual hydrogen content in specimens with hydrogen flakes, in order to confirm the results of the limited number of tests achieved so far. For example, the licensee has estimated an upper bound on the amount of residual hydrogen that might still be present in the flaws. The licensee shall demonstrate that the chosen material properties are still valid, even if the upper bound quantity of hydrogen would still be present in critical flaws.*

## Steps taken

A test program was carried out on the Doel 3 RPV H1 nozzle shell cut-out and on block VB395/1 to measure the residual hydrogen in the metal. Approximately 100 analyses were carried out on samples taken from different positions. The following tests were performed:

- Melt extraction to measure the total amount of hydrogen.
- Measurement of diffusible hydrogen by heating at 300 °C.
- Thermal desorption spectroscopy by gradual heating at different heating rates in the temperature range of 300 to 600 °C, to determine the trapping behaviour.

In addition, the amount of hydrogen present inside flakes was investigated. Hot extraction at 900 °C and at 1100 °C was performed to evaluate if hydrogen is still present inside the flakes, by comparing samples with flakes to samples without flakes.

## Conclusions

The total hydrogen is at the same level for the two test materials. There is no diffusible hydrogen found and the residual hydrogen is trapped.

After the additional investigation requested by the FANC, it is confirmed that there is no significant amount of hydrogen present inside flakes.

Since all the measured values for specimens with or without flakes are well below 0.8 ppm (the threshold value found in literature), no adverse effect of hydrogen on the material properties is to be expected.

# 3.4 Representativeness of the AREVA Shell with regard to RPV Flaking

The representativeness of the AREVA shell VB395 regarding hydrogen flaking has been confirmed. Therefore, the findings and conclusions of the tests on the AREVA shell can be transferred to the RPVs.

The hydrogen flaking in the AREVA shell VB395 is representative for the flaking in the Doel 3 and Tihange 2 RPVs, for the following reasons:

- The UT inspection shows similar flaw characteristics (average size larger than average size measured in both RPVs and average density of 23 indications per litre, which is comparable to the maximum density in the two RPVs), and a similar position versus the macro-segregation.
- Chemical and micro-structural characteristics are similar, more particularly, the macro-segregation and ghost lines features. This was also confirmed by a comparison with the Doel 3 RPV H1 nozzle shell cut-out.
- The presence of hydrogen and trapping behaviour are similar.
- The flaking root causes are similar.

Therefore, the findings and conclusions of the tests on the AREVA shell can be transferred to the RPVs.

# 4 Material Properties

## 4.1 Effect of Ghost Lines on Mechanical Properties

Tests performed on specimens from the Doel 3 H1 nozzle cut-out show that the ghost lines have no significant effect on the Charpy impact or fracture toughness properties.

### Requirement

The following covers the mechanical testing part of this long-term requirement:

> *The licensee shall further investigate experimentally the local (micro-scale) material properties of specimens with macro-segregations, ghost lines and hydrogen flakes (for example local chemical composition). Depending on these results, the effect of composition on the local mechanical properties (i.e. fracture toughness) shall be quantified.*

### Steps taken

To answer this requirement the following tests and analysis were performed on specimens taken from the Doel 3 H1 nozzle cut-out:

- **Charpy impact tests**

  Twelve Charpy impact specimens were taken with the notch at the level of a ghost line (crack propagation perpendicular to the plane of the ghost line). No difference is seen in the Charpy-impact test as compared to the curves established for the material free of ghost lines.

- **Fracture toughness tests**

  Eighteen fracture toughness tests were performed on pre-cracked Charpy specimens tested in three-point bending in the same orientation as the Charpys (sixteen tests in the transition and two in the ductile domain). The crack tip was positioned in the ghost line. Again, no significant difference is seen as compared to specimens without ghost lines. Scanning Electron Microscope analyses were performed on all fracture surfaces of the pre-cracked Charpy specimens. This confirmed the presence of zones of intergranular fracture at the crack front, which shows that the crack tip was well located within the ghost line. Other analyses, such as a chemical analysis, confirmed this finding.

- **Tensile tests**

  Three tensile tests were performed at 290 °C on specimens with a ghost line parallel to the specimen axis and on specimens with a ghost line perpendicular to the specimen axis.

  - For the tests with the ghost line perpendicular to the axis, the specimen broke outside of the ghost line. This is logical considering the higher yield stress of the ghost line.
  - For the specimens with the ghost line parallel to the specimen axis, the yield stress increases and the total elongation is reduced.

### Conclusion

These analyses show that there is no significant effect of the ghost lines on the Charpy impact or fracture toughness properties.

# 4.2 Effect of Hydrogen Flakes on Material Properties

Tensile tests on specimens taken from the VB395 shell show that the ductility of the material in the ligaments between flakes is similar to the ductility of the material free of flakes. Large-scale tests on material containing flakes confirm the good ductility and load bearing capacity.

The fracture toughness tests confirm that the 50 °C shift of $RT_{NDT}$ considered in the Safety Case is appropriate to cover the potential deterioration of the local fracture toughness properties in the vicinity of the hydrogen-induced flaws.

## Requirement

In 'Doel 3 and Tihange 2 reactor pressure vessels – Provisional evaluation report (30 January 2013)', the FANC requires the following with regard to the material test program:

> *The licensee shall complete the material testing program using samples with macro-segregations containing hydrogen flakes. This experimental program shall include:*
>
> *- small-scale specimen tests:*
>
> *- local toughness tests at hydrogen flake crack tip*
>
> *- local tensile tests on ligament material near the flakes*
>
> *- large-scale (tensile) specimen tests*

## Steps taken

An extensive testing program was performed on different blocks extracted from the VB395 shell, both in a zone free of flakes (as reference) and in a zone affected by flakes. A total of 172 specimens of different types were tested.

Figure 4.1: Blocks from AREVA shell VB395

- **Tensile tests**

  A large number of tensile tests (6.25 mm diameter) were performed in different orientations in the ligament between hydrogen flakes. These tests confirmed that the ductility of the material in the ligaments between flakes is similar to the ductility of the material free of flakes. The results were confirmed by tests on large specimens (18.75 mm and 25 mm diameter) containing hydrogen flakes roughly parallel to the specimen axis.

- **Fracture toughness tests**

  The fracture toughness tests confirm that the 50 °C shift of $RT_{NDT}$ considered in the Safety Case is appropriate to cover the potential deterioration of the local fracture toughness properties in the vicinity of the hydrogen-induced flaws.

  - **Fracture toughness tests were performed on the reference material and on the ligament between flakes.** The results show a slightly lower fracture toughness for the ligaments, which corresponds to an increase of the Master Curve Reference Temperature $T_0$ of 11 °C. Although this difference is comparable to the experimental scatter, it is conservatively considered as a real effect indicative of a slightly reduced fracture toughness in the ligaments.
  - **Fracture toughness tests were performed on specimens with a hydrogen flake as crack initiator** (in place of the usual fatigue crack), as shown on the figure below. The preparation of such specimens is complex and these tests do not fulfil the standard requirements in terms of crack front regularity, however the measured values are confirmed by 3D Finite Element Analysis. The test results are close to the ones obtained on the ligament between flakes, with an increase of the Master Curve Reference Temperature $T_0$ of the order of 14 °C.

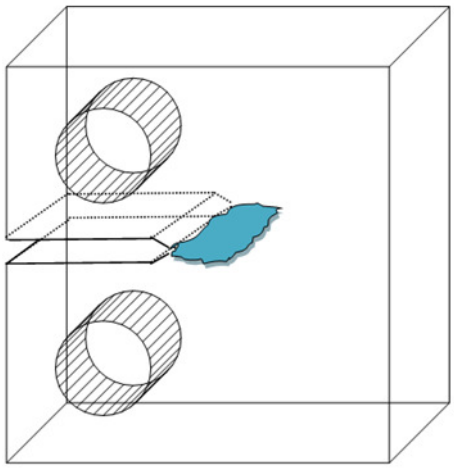

**Figure 4.2: CT12.5 specimen with a hydrogen flake at the crack tip for direct measurement of toughness at the tip of the flake**

The total shift in $RT_{NDT}$ is the sum of 11 °C, 14 °C, and a value between 4 to 12 °C (corresponding to the spatial fluence variation in the RPV for the most critical flaw locations), covering a possibly higher irradiation embrittlement sensitivity of the macro-segregated zone. This total (between 29 and 37 °C) is well within the 50 °C margin on the $RT_{NDT}$ considered in the Structural Integrity Assessment.

## Conclusions

- The fracture toughness properties of the material in the ligament between flakes are comparable to the properties of the material in the zone free of flakes.
- The fracture toughness tests on specimens with hydrogen flakes as crack initiator (instead of the usual fatigue crack) are not strictly valid according to the standard, but can nevertheless be used. They confirm that there is limited difference with the specimens taken from the ligaments between flakes.

- All results are compared in the figure below. For clarity only the Master Curves for the specimens taken in the ligaments between flakes are represented. All results are enveloped by the ASME curve indexed on the $RT_{NDT}$ of this material, except for two points at very low temperature (-115 °C), which are not relevant with regard to operating conditions.
- The surveillance results for the Doel 3 and Tihange 2 RPVs have shown that the effect of embrittlement, as evaluated by the FIS formula, is conservative. This led to a margin of 10 to 25 °C which is not taken into account in the evaluation.
- The results confirm the conservativeness of the 50 °C margin on $RT_{NDT}$ considered in the structural integrity analyses.

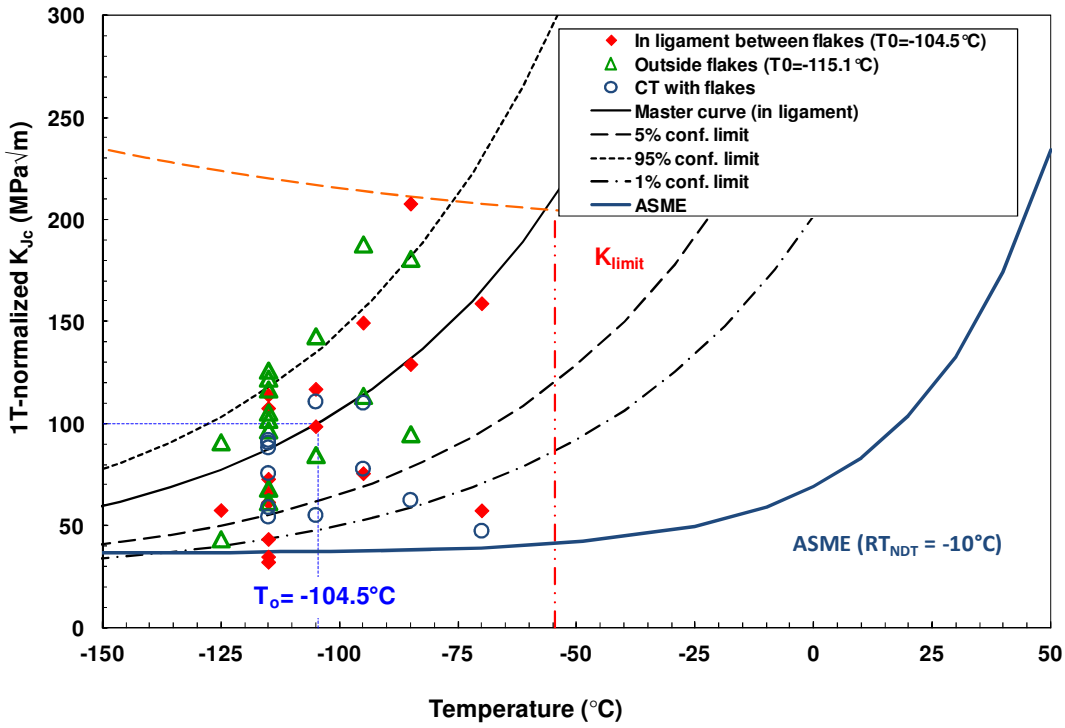


**Figure 4.3: Comparison of fracture toughness of the VB395/61 material in the ligament between flakes and in the material free of flakes**

# 5 Structural Integrity

## 5.1 ASME III Elasto-Plastic Analysis

After the ASME III NB-3228.3 elasto-plastic analysis, it is shown that the collapse load evaluated for the most penalizing flaw configuration meets the acceptance criterion.

### Additional analysis

During the discussions of the Safety Case Report, it was decided to conduct an additional elasto-plastic analysis according to the rules of ASME III NB-3228.3.

To determine the collapse load, an elasto-plastic analysis was performed for the lower and upper core shells of the Doel 3 RPV. The analysis also covers the transition ring, the nozzle shell, and the vessel flange, where fewer flaws have been detected.

The results of the analysis show that the collapse load evaluated for the most penalizing flaw configuration meets the acceptance criterion of ASME III NB-3228.3.

## 5.2 Flaw Acceptability Analysis Core Shells

The Flaw Acceptability Analysis was expanded with a flaw-screening criterion approach. Only eleven flaws or groups of flaws in the Doel 3 RPV exceed this screening criterion. However, they meet the acceptability criterion. Additional refined analyses show substantial margins.

### Requirement

To assess the effects of the high number of detected flaws, Bel V proposed to use a deterministic screening criterion approach. The objective of this approach is to show:

- That the hydrogen-induced degradation does not significantly affect the safety level of the RPVs.
- That only a limited number of flaws require a more in-depth analytical evaluation.

### 5.2.1 Screening Approach integrated into the Flaw Acceptability Analysis

The screening criterion approach has been developed and integrated in the Flaw Acceptability Analysis of the RPV core shells, as shown in this figure and outlined below:

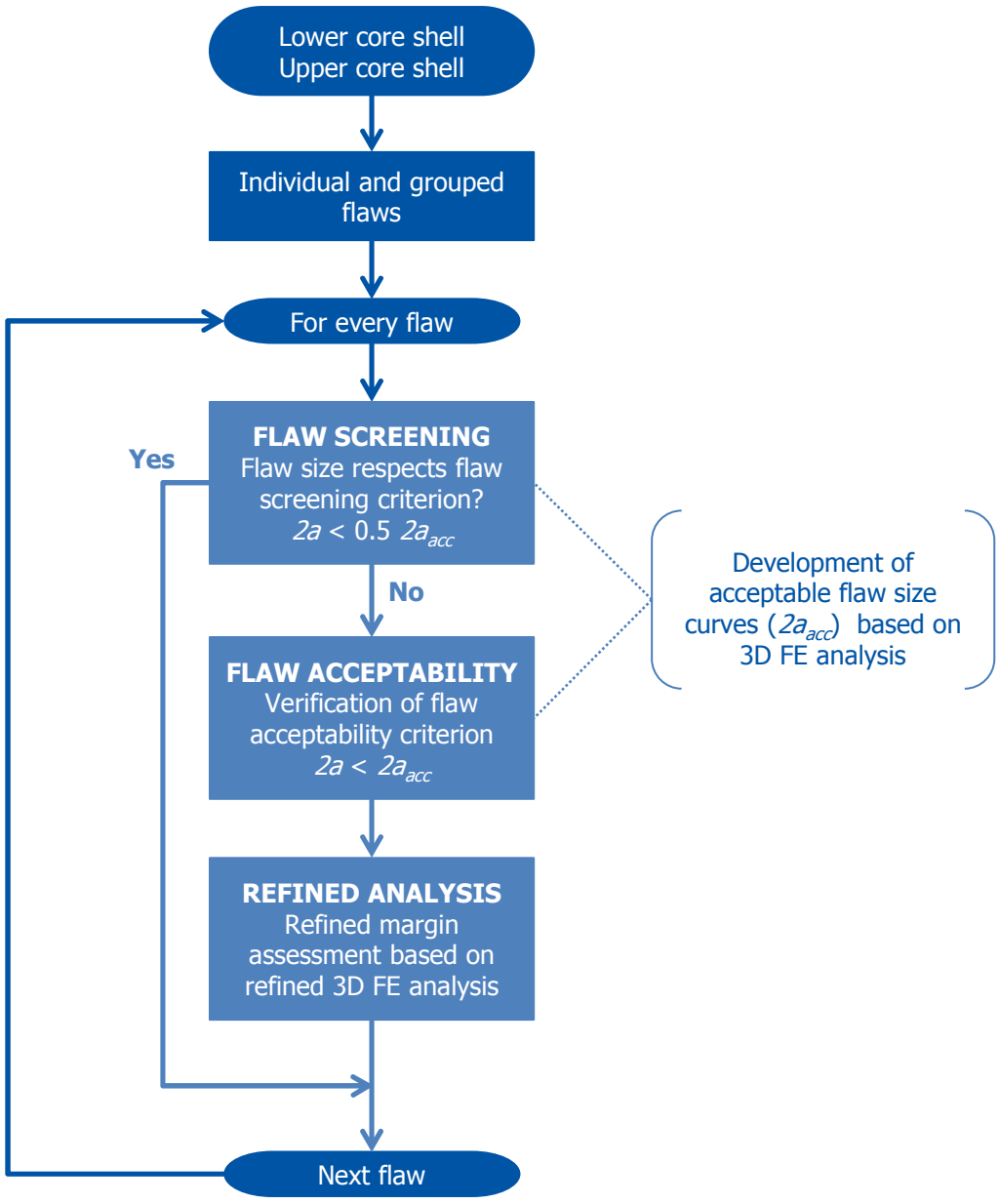


**Figure 5.1: Schematic overview of Flaw Acceptability Analysis for core shells**

## 5.2.2 Flaw Screening

The flaw-screening criterion is based on the acceptable flaw size $2a_{acc}$. The screening is a graded approach that identifies only a limited number of flaws requiring a more in-depth analytical evaluation. The flaws are screened as follows:

- Closely spaced flaws are grouped based on grouping rules, as in the Safety Case Report.
- Each individual flaw or group of flaws is submitted to the flaw-screening criterion:
  - **If flaw size 2a is less than half of the acceptable flaw size $2a_{acc}$,** then flaw is considered to be harmless and no further analysis is required.
  - **If flaw size 2a is larger than half of the acceptable flaw size $2a_{acc}$,** further analysis is required.

Applying the flaw-screening criterion to the flaws detected in the RPV core shells of Doel 3 shows that eleven flaws (isolated or grouped) exceed the flaw-screening criterion, as illustrated here:

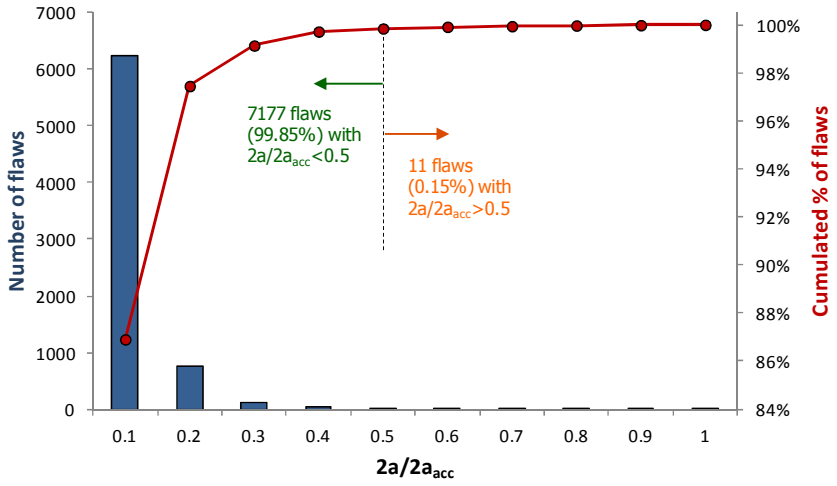


**Figure 5.2: Flaw-screening criterion applied to core shells of Doel 3**

These eleven flaws require further analysis according to Figure 5.1.

## 5.2.3 Flaw Acceptability

The eleven flaws exceeding the flaw screening criterion need further analysis, which means that it is verified whether or not flaw size 2a remains below the acceptable flaw size $2a_{acc}$ for particular combinations of inclinations and $RT_{NDT}$ values (see Safety Case Report, Chapter 4.8.3 Deterministic SIA). Also, an additional shift of 50 °C in $RT_{NDT}$ is considered, covering the effect of macro-segregations on the fracture toughness properties of the base metal.

The result of this analysis is given in Figure 5.3, which gives the ratio $2a/2a_{acc}$ for each of the flaws. Ten flaws are located in the lower core shell, only one (labelled GP0159) is located in the upper core shell. **Based on Figure 5.3 it can be concluded that the eleven flaws exceeding the screening criterion meet the acceptability criterion ($2a < 2a_{acc}$).**

**Acceptable flaw size**

The acceptable flaw size $2a_{acc}$ is determined from the acceptable flaw size curves that give for particular combinations of inclinations and $RT_{NDT}$ values the acceptable flaw size as a function of the ligament (see Safety Case Report, Chapter 4.8.3 Deterministic SIA). These curves have been determined from numerous 3D finite element simulations of the flaw behaviour in the RPV wall.

The $RT_{NDT}$ considered at the flaw's location is the $RT_{NDT}$ at the end of the service lifetime plus an additional shift of 50 °C that to cover the potential deterioration of the local fracture toughness properties in the vicinity of the hydrogen-induced flaws.

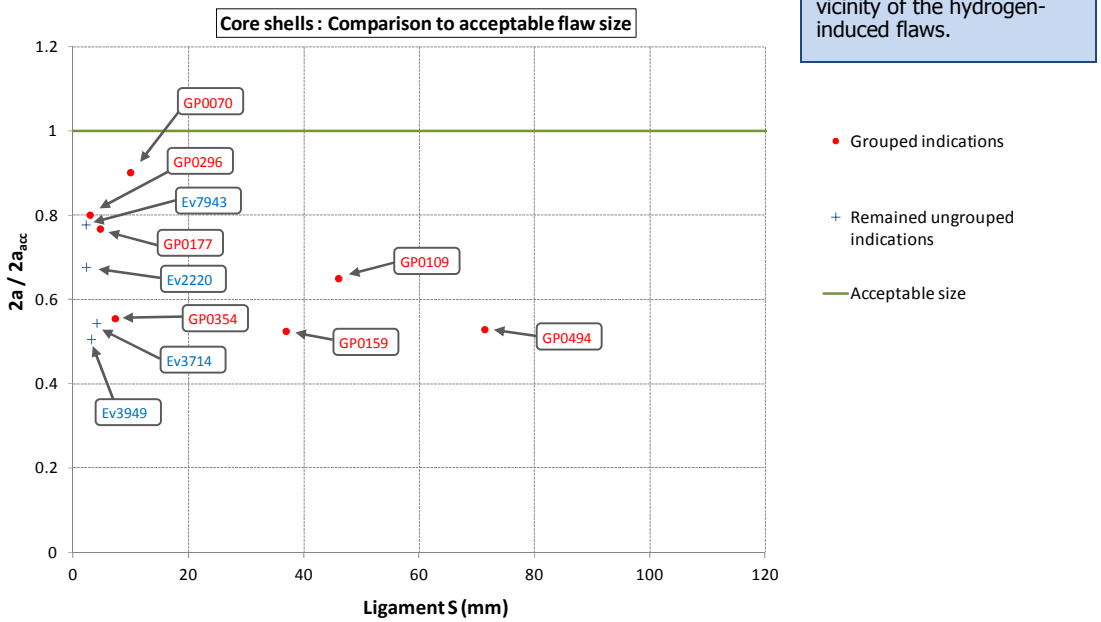


**Figure 5.3: Ratio $2a/2a_{acc}$ as a function of ligament for flaws exceeding the screening criterion**

In the above figure, grouped flaws are labelled by 'GP' followed by the flaw number. Individual flaws are labelled by 'Ev' followed by the flaw number.

## 5.2.4 Refined Analysis

Once concluded that the flaws are acceptable, the actual margins of each flaw and group of flaws are assessed. This is done through 3D Finite Element (FE) analysis of grouped and individual flaws, in the following way:

### Refined analysis of grouped flaws

- The grouped flaw is ungrouped into individual flaws.
- Each individual flaw is modelled as an elliptical flaw fitting in the rectangular box surrounding the UT indication, and not as a circular flaw enveloping this elliptical flaw.
- A 3D Finite Element analysis is performed covering all individual flaws in the group and their mutual interaction.
- For each flaw, the actual maximum Stress Intensity Factor $K_{eq,max}$ is determined.

As an example, Figure 5.4 illustrates the analysis of the grouped flaw GP0070 depicted in Figure 5.3. The margin with respect to the acceptable flaw size increases from 10% for the grouped flaw approach to more than 75% when considering a 3D analysis of the multiple flaw configuration. Also given in this figure are the inclinations and flaw diameters considered for the grouped flaw on one hand and for the individual flaws on the other hand.

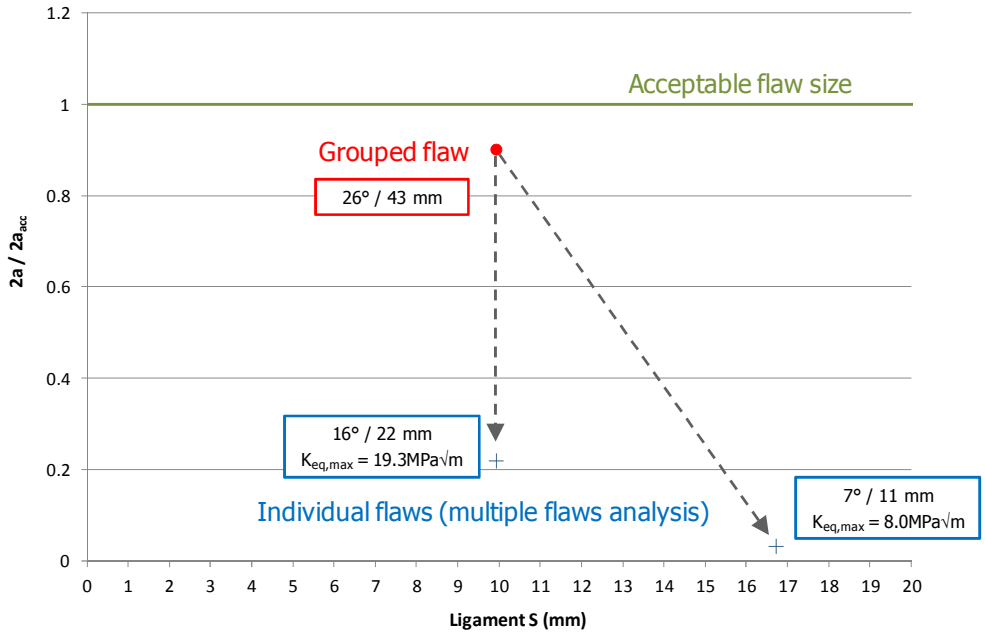


**Figure 5.4: Refined analysis of grouped flaw GP0070**

### Refined analysis of individual flaws

- The actual neutron fluence was used at the location of the flaws.
- The vicinity of individual flaws has been considered in detail in order to account for the interaction with potential surrounding flaws. Where applicable, interactions with neighbouring flaws were taken into account, even if these interactions are lower than the 6% considered in the grouping criteria.
- Elliptical flaws are considered, instead of circular flaws.
- A Safety Injection (SI) water temperature of 30 °C is considered. As described in the Safety Case Report, Electrabel voluntarily decided to increase the temperature of this water from 7 °C to 30 °C. This will reduce the temperature gradient of the inner RPV surface in case of Pressurized Thermal Shock (PTS).

## Results of both refined analyses

Refined analyses were performed for six flaw configurations. These six configurations had the smallest margins with respect to the acceptable size, and were representative for the eleven flaw configurations exceeding the flaw screening criterion (see Figure 5.3):

- Grouped flaws: GP0070, GP0296, GP0177, GP0494.
- Individual flaws: Ev7943 and Ev2220.

The results are summarized here:

| Nr. | $2a/2a_{acc}$ | Refined $2a/2a_{acc}$ | $K_{eq,max}$ (MPa√m) |
|---|---|---|---|
| GP0070 | 0.90 | 0.22 | 19.3 |
| GP0296 | 0.80 | 0.28 | 20.5 |
| EV7943 | 0.78 | 0.44 | 25.0 |
| GP0177 | 0.77 | 0.27 | 20.5 |
| EV2220 | 0.68 | 0.39 | 29.2 |
| GP0494 | 0.53 | 0.09 | 4.6 |

**Table 5.1: Refined analysis of flaw configurations exceeding the flaw-screening criterion**

The column 'Refined $2a/2a_{acc}$' gives the ratio $2a/2a_{acc}$ as determined under the refined analysis described above. The last column gives the actual maximum Stress Intensity Factor (SIF) $K_{eq,max}$. All SIF values are below the lower bound fracture toughness values of the ASME curves.

From the results of the analyses, it can be concluded that substantial additional margins are obtained for the grouped flaws (at least 70%) and the individual flaws (at least 40%). For the five other flaw configurations similar conclusions may be drawn.

Finally, the $2a/2a_{acc}$ ratios for all flaws in the core shells of the Doel 3 RPV, including the results of the refined analyses, are represented in the following plot as a function of the flaw ligament.

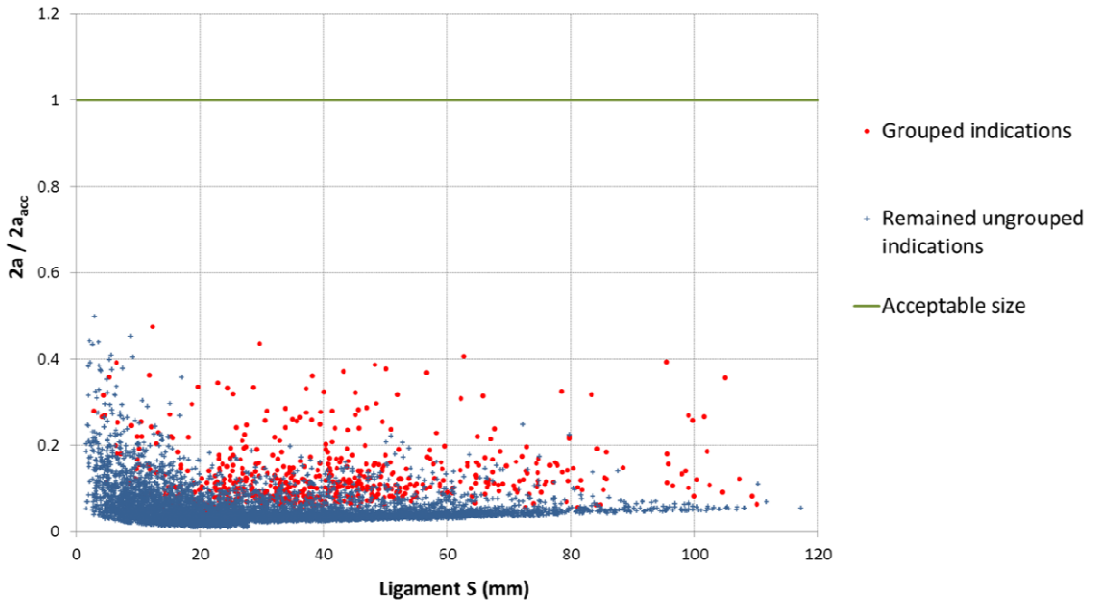


**Figure 5.5: Core shells, comparison to acceptable flaw size**

## Conclusion

As shown in Figure 5.5, all flaws (isolated or grouped) have substantial margin with respect to the acceptability criterion.

# 5.3 Sensitivity Analyses

## 5.3.1 Sensitivity Analysis of the Structural Integrity Assessment (SIA) with Respect to Ligament

A number of sensitivity analyses were performed on the most penalizing flaw of the two RPVs (Doel 3 flaw Ev2220), considering effects such as the ligament tending to zero, a 5° larger inclination, the actual fluence, the flaw shape, and the Safety Injection water temperature. Results confirm that a significant margin remains in all cases.

### Requirement

The International Expert Review Board (IERB) required a sensitivity analysis for the location of the flaws in the structural analysis. More specifically, the IERB suggested considering the most critical flaw of the analysis (the Doel 3 flaw Ev2220) and to investigate how the results of the SIA change when the flaw's ligament S would tend to zero.

### Conclusion

A number of sensitivity analyses were performed on the most penalizing flaw of the two RPVs (Doel 3 flaw Ev2220), considering effects such as the ligament tending to zero, a 5° larger inclination, the actual fluence, the flaw shape, and the Safety Injection water temperature. Results confirm that a significant margin remains in all cases. The figure below shows the evolution of the margin with respect to the acceptability criterion with the ligament S tending to zero.

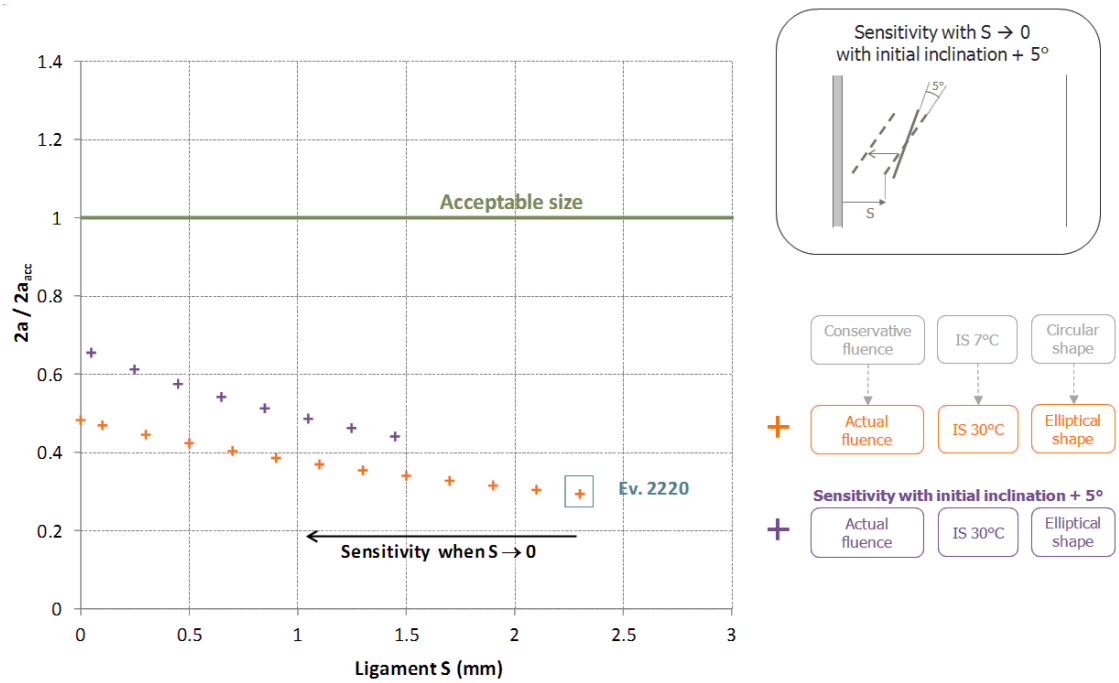


**Figure 5.6: Sensitivity analysis for S→0 combined with effect of a 5° increase of the inclination of the Doel 3 flaw (Ev2220)**

## 5.3.2 Sensitivity Study of Higher Tilted Flaws

The integration of potentially unreported flaws with an inclination up to 20° in the Structural Integrity Assessment of the lower core shell of Doel 3 does not affect its structural integrity.

### Related action: potentially unreported higher tilted flaws

Chapter 2.1.4 of this addendum, Potentially Unreported Higher Tilted Flaws, addresses the question of flaws that could potentially be present in the RPV wall, but would not have been taken into account in the structural integrity analysis. This is because the amplitude of their UT response would have been below the reporting level applicable during the 2012 UT inspections of the Doel 3 RPV.

The outcome of this action is the solid blue line in the figure below. It is an envelope curve that defines the size of the largest flaw with a 20° inclination that would potentially not have been reported, as a function of the position in the RPV wall in the depth range between 25 and 120 mm.

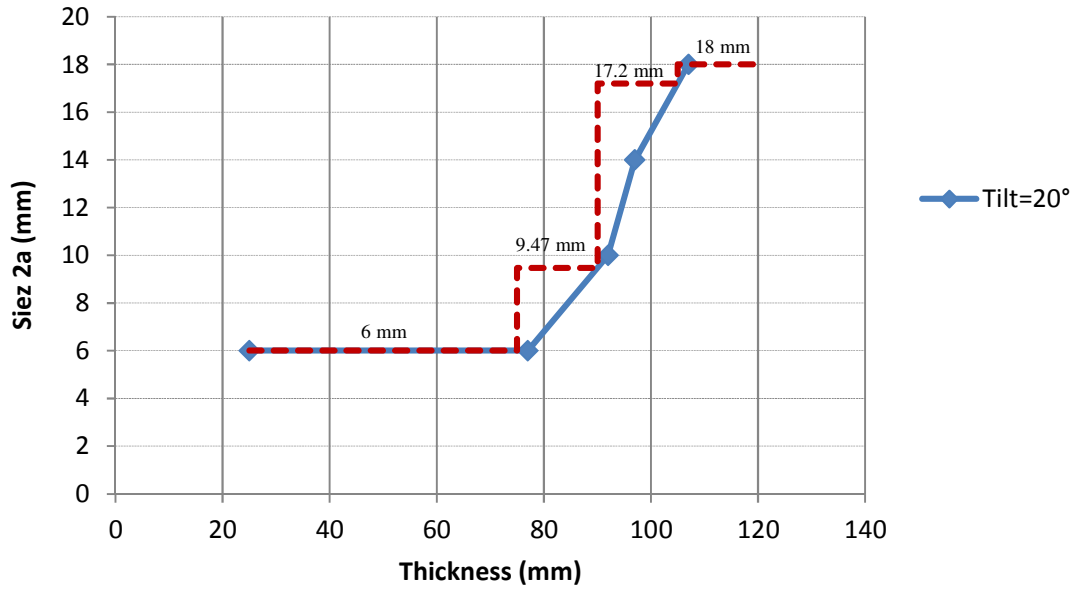


**Figure 5.7: Size of largest potentially unreported higher tilted flaw (20° tilt)**

### Requirement

In 'Doel 3 and Tihange 2 reactor pressure vessels – Provisional evaluation report (30 January 2013)', the FANC requires the following with regard to potentially unreported flaws and structural integrity:

> *Taking into account the results of the actions related to the previous requirement on the detection of higher tilt defects during in-service-inspections, the licensee shall evaluate the impact of the possible non-reporting of flaws with higher tilts on the results of the structural integrity assessment.*

## Steps taken

This action addresses the impact that potentially unreported flaws (see Chapter 2.1.4 Potentially Unreported Higher tilted Flaws) could have on the results of the Structural Integrity Assessment (SIA), if they were to be included. The analysis was accomplished by adding a population of potentially unreported flaws to the reported flaws. SIA is then applied to all detected and potentially unreported flaws.

The action was carried out for the lower core shell of Doel 3, the component most affected by hydrogen flaking:

- The depth range of 25-120 mm is divided into four intervals. For each interval, a bounding maximum flaw size is conservatively determined, as illustrated in Figure 5.7 by the red dashed line. All potentially unreported flaws in a particular interval are given the maximum inclination of 20°.
- In total, 1045 potentially unreported flaws were considered. They have been distributed into the shell similar to the reported flaw distribution.
- Finally, the Flaw Acceptability Analysis, as outlined in Chapter 5.2, was performed on the entire population of reported and potentially unreported flaws.

## Conclusion

From the analysis, it can be concluded that the integration of potentially unreported flaws in the SIA of the lower core shell of Doel 3 does not affect its structural integrity: the maximum ratio $2a/2a_{acc}$ remains below the flaw acceptability criterion.

### 5.3.3 Flaw Acceptability Analysis including DTRs of Doel 3

The integration of DTRs (clad interface imperfections) as hydrogen flakes in the Structural Integrity Assessment of the Doel 3 RPV does not affect its structural integrity.

In addition to the hydrogen flakes, the RPV UT inspections also revealed indications located at the interface between cladding and base metal, referred to as clad interface imperfections (French: *défauts technologiques de revêtement* or DTR). In Doel 3, 320 DTRs were found. The majority of DTRs were located in the lower core shell, which also is the shell in which the cloud of hydrogen flakes is situated close to the cladding-base metal interface.

Therefore, although the DTR indications were confirmed not to be hydrogen flakes, it was verified in which way the SIA conclusions for this shell would change if the DTRs would be considered as additional hydrogen flakes (pseudo-hydrogen flakes).

The SIA of the Doel 3 core shells was performed again on the full population of reported hydrogen flakes and the 320 pseudo-hydrogen flakes. For the flakes above the screening criterion, a refined analysis was performed, which demonstrates that the pseudo-hydrogen flakes have no impact on the maximum $2a/2a_{acc}$ ratio.

A **DTR** is any flaw located at the cladding-base metal interface, parallel to the vessel surface, that does not penetrate the base metal itself. A DTR should not be confused with underclad cracks (French: défauts sous revêtement or DSR), which are planar flaws at the cladding-base metal interface, oriented perpendicular to the RPV surface and generated by cold cracking. No underclad cracks were discovered during the 2012 inspections.

# 5.4 Large-Scale Validation Testing

The material's good ductility and load bearing capacity was demonstrated by the tensile tests described in the previous chapter. These tests confirmed that the ductility of the material in the ligaments between flakes is similar to the ductility of material free of flakes.

The two large-scale tensile specimens with inclined flakes tested at room temperature exhibited significant uniform elongation and local plasticity at crack tips. The results clearly indicate the good ductility and load bearing capacity.

The 3D Finite Element analysis on two large-scale tensile specimens with inclined flakes tested at -80 °C, demonstrated that the specimen failure was as predicted by fracture mechanics, and that there is no premature brittle fracture.

The 3D Finite Element simulation of two large-scale bend bars with flakes tested in four-point bending demonstrated that the failure load calculated according to the same methodology as applied in the Structural Integrity Assessment of the RPVs was significantly lower than the actual failure load.

### Requirement

In 'Doel 3 and Tihange 2 reactor pressure vessels – Provisional evaluation report (30 January 2013)', the FANC requires the following with regard to large-scale validation testing:

> *The licensee shall complete the ongoing test program by testing larger specimens containing hydrogen flakes, with the following objectives:*
>
> *Objective 1: Tensile tests on samples with (inclined) multiple hydrogen flake defects, which shall in particular demonstrate that the material has sufficient ductility and load bearing capacity, and that there is no premature brittle fracture.*
>
> *Objective 2: An experimental confirmation of the suitability and conservatism of the 3D finite elements analysis.*

## 5.4.1 Objective 1

### Steps taken

Tensile tests were performed on four large specimens (25 mm diameter) from the VB395 shell. The four specimens contained multiple hydrogen flakes with an inclination of 20° with respect to the axis of the specimen.

Two specimens were tested at room temperature, while the other two were tested at -80 °C.

### Conclusions

These tests cannot be interpreted as normal tensile tests, because the specimens' behaviour is mainly determined by stress concentrations at the tip of the flake (governed by the laws of fracture mechanics) and not by the material's plasticity. However, the two specimens tested at room temperature exhibited significant uniform elongation and local plasticity at crack tips, confirming their ductility and load bearing capacity.

Also, the material's ductility and load bearing capacity was demonstrated by the tensile tests described in Effect of Hydrogen Flakes on Material Properties (4.2). These tests confirmed that the ductility of the material in the ligaments between flakes is similar to the ductility of the material free of flakes.

## 5.4.2 Objective 2

### Steps taken: overview

The suitability and conservativeness of the 3D Finite Element (FE) analyses on which the Safety Case relies, is demonstrated by simulating and predicting the outcome of the following tests:

- A four-point bending test applied to bars with hydrogen flakes (from block VB395/62).
- Tensile tests on four large specimens taken from the VB395 shell. The specimens contained multiple hydrogen flakes with an inclination of 20° with respect to the axis of the specimen (see also Objective 1).

### Four-point bending test of bars with hydrogen flakes

The Structural Integrity Assessment demonstrated that the Doel 3 RPV shells meet the required margins against crack initiation for all operating conditions. This means that any experiment that is fully representative of the real configuration and loading conditions of the RPV shells will never lead to brittle crack initiation, even when not assuming a fracture toughness value at the lower bound of the ASME curve. Therefore, test conditions must be more severe. Preliminary analyses showed that more severe conditions can be obtained by subjecting a bend bar of 30x60x260 mm with a surface-breaking flaw in the high-stress region to a four-point bending test at a temperature as low as -130 °C (see Figure 5.8).

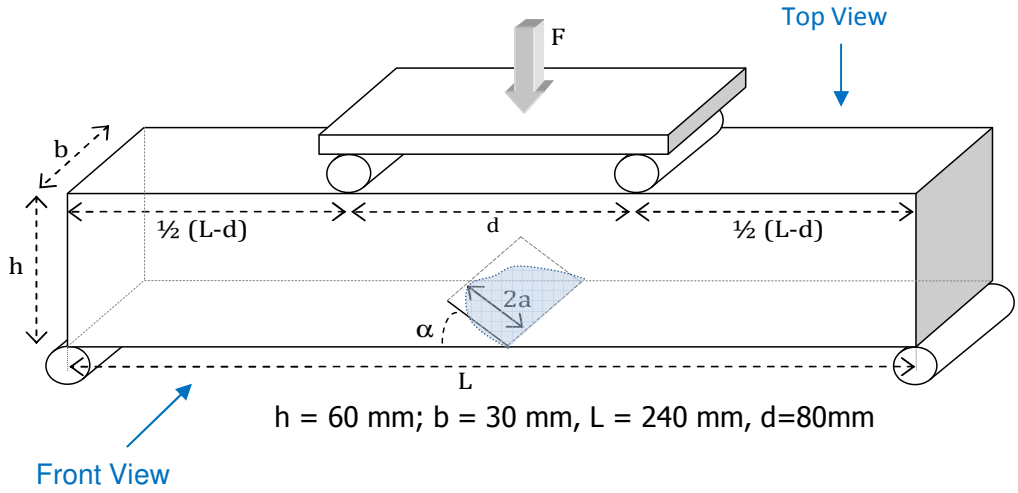


**Figure 5.8: Four-point bend specimen with surface breaking flake**

Two bend bars containing several flakes and a least one surface-breaking flake covering the whole width of the specimen, were extracted from the VB395/62 block.

The failure load was calculated based on a 3D Finite Element simulation of the bend bars and according to the same methodology as applied in the SIA of the RPVs. This means that each flaw is modelled as having the largest inclination and size possible within the volume (box) defined by the UT inspection. In addition, the lower bound fracture toughness curve is considered in the analysis. The simulated failure loads were communicated to the Safety Authorities before performing the tests.

The actual four-point bending tests yielded failure loads well above the predicted values, and hence confirmed the conservativeness of the analysis:

| Specimen | Calculated Failure Load | Experimental Failure Load |
|---|---|---|
| Specimen 1 | 111 kN | 209 kN |
| Specimen 2 | 79 kN | 489 kN |

**Table 5.2: Comparison predicted and experimental failure load**

The large difference between calculated and experimental failure load for the second specimen is due to the fact that the real flake is considerably smaller and less inclined as compared to the modelled flake. Taking into account the actual dimension and inclination of the flake, a new simulation yielded a calculated failure load of 189 kN which is much closer to but still below the experimental failure load.

## Large tensile tests performed on specimens with multiple inclined hydrogen flakes

Tensile tests were performed on four large specimens (25 mm diameter) taken from the VB395 shell. The specimens contain multiple hydrogen flakes oriented at 20° with respect to the specimen axis as shown in Figure 5.9.

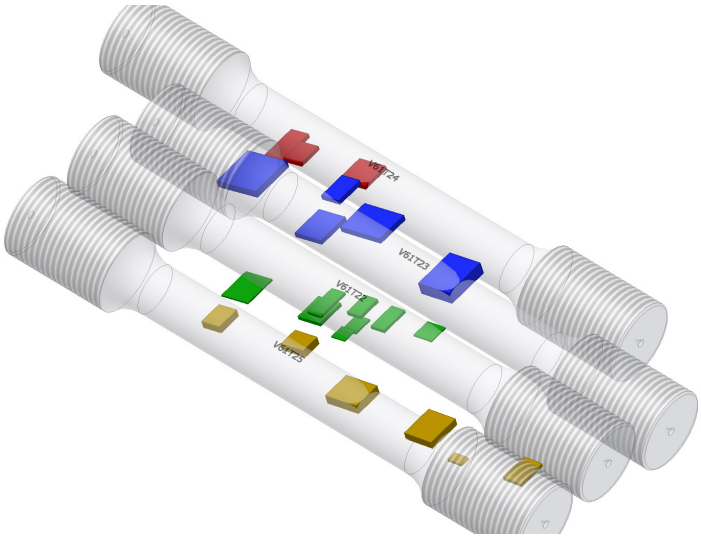

**Figure 5.9: 3D view of the tensile test specimens with flakes tilted 20° with respect to specimen axis. The flakes are represented by coloured boxes that envelope the actual flakes.**

The two specimens tested at room temperature broke after plastic deformation (3% and 5.3% uniform elongation). Since SIA is performed in the elastic domain, these tests are not used for validation of the 3D Finite Element Analysis.

The two specimens tested at -80 °C broke shortly after reaching the (engineering) yield stress at this temperature (600 MPa), without significant gross plastic deformation. A detailed 3D Finite Element analysis demonstrated that there is no premature brittle fracture and that the specimen fracture was predictable.

In both specimens tested at -80 °C, the equivalent stress intensity factor at the tip of the flake where the failure occurred was well above the lower bound fracture toughness. This means that the actual fracture occurred at a load well above the calculated failure load and at the location predicted by the 3D Finite Element Analysis. This demonstrates once more that the 3D Finite Element analysis is conservative with respect to the experiments.

### Conclusions

Two large-scale tests were performed on bend bars tested in four-point bending. In both cases, the failure load was significantly higher than the failure load calculated as during the SIA of the RPVs.

The 3D Finite Element analysis on the two large-scale tensile specimens with flakes tested at -80 °C demonstrated that the specimen failure was as predicted by fracture mechanics, and that there is no premature brittle fracture.

# 5.5 Conservativeness

The conservativeness of the Fatigue Crack Growth (FCG) methodology is demonstrated through an additional analysis based on the actual orientations of the flaws and groups of flaws, also taking into account a more recent edition of the ASME XI.

Computational Fluid Dynamics (CFD) simulations and mock-up tests demonstrate the conservativeness of the Axisymmetric Thermal Loading method, as applied in the Safety Case.

## 5.5.1 Conservativeness Embedded in Fatigue Crack Growth Analyses

### Additional analysis

The Fatigue Crack Growth (FCG) analyses of the flaws detected in the Doel 3 RPV are based on:

- Conservative assumptions regarding the numbers of transients and heat transfer from primary water to the RPV wall.
- A conservative approach considering the axial and circumferential projections of flaws rather than their actual orientations.

An additional analysis has been performed to illustrate the conservativeness of the methodology that is based on the actual orientations of the flaws and groups of flaws rather than on their axial and circumferential projections. This analysis also takes into account a more recent edition of the ASME XI.

Even when maintaining conservative assumptions regarding numbers of transients and heat transfer, the new calculation showed a negligible growth of 0.41%, far below the values considered in the Safety Case Report (1.72%).

## 5.5.2 Conservativeness of Axisymmetric Thermal Loading in case of Cold Water Injection following LOCA

### Additional analysis

Among the various transients considered in the Pressurized Thermal Shock (PTS) analysis included in the Safety Case, the most penalizing is the Loss-Of-Coolant Accident (LOCA). During this, the Safety Injection system starts to inject cold borated water in the three cold legs.

Under very specific conditions, the cold water injected in the cold legs could result in a stratification in the cold legs. When the injected cold water enters the downcomer area, part of it is flowing on the core barrel and part along the RPV wall. The cold water entering the downcomer leads to the plume effect, which generates a non-axisymmetric temperature distribution in the downcomer and a non-axisymmetric thermal loading of the RPV wall.

In the Safety Case, the plume effect was not considered. Instead, a conservative axisymmetric temperature distribution was taken into account. Bel V asked to address the issue that an axisymmetric distribution of the thermal loads (without plume effect) could not be the most detrimental distribution for the detected flaws.

### Conclusion

The plume effect has been thoroughly investigated through Computational Fluid Dynamics (CFD) simulations and through mock-up tests demonstrating that the fracture mechanics assessment of the RPV based on a sufficiently conservative axisymmetric temperature distribution, as applied to the Doel 3 RPV, is justified.

# 6 Load Tests

The Doel 3 RPV was subjected to a load test with acoustic emission (AE) measurements, followed by a post-load UT inspection.

The AE measurements performed did not reveal any source or area for which complementary investigations are required.

The number of flaw indications reported by the post-load test inspection is fully consistent with the findings of the 2012 RPV inspection. The peak amplitude and dimensions of every indication reported by the post-load test inspection match those of the 2012 RPV inspection.

All examination results confirm that the load test did not modify the condition of the material.

## Requirement

In 'Doel 3 and Tihange 2 reactor pressure vessels – Provisional evaluation report (30 January 2013)', the FANC requires the following with regard to potentially unreported flaws and structural integrity:

> *In addition to the actions proposed by the licensee and the additional requirements specified by the FANC in the previous sections, the licensee shall perform a load test of both reactor pressure vessels. The objective of the load test is not to validate the analytical demonstration on the reactor pressure vessel itself but to demonstrate that no unexpected condition is present in the reactor pressure vessels. The methodology and associated tests (acoustic emission and ultrasonic testing...) will be defined by the licensee and submitted to the nuclear safety authority for approval. The acceptance criterion will be that no crack initiation and no crack propagation are recorded under the pressure loading.*

# 6.1 Definition of Test Conditions

The **Acoustic Emission (AE) technique** is a non-destructive technique that has been widely used in industry for more than 30 years. It is based on the principle that flaws that propagate under mechanical stress (e.g. due to internal pressure) undergo local micro-displacements that release energy in the form of transient elastic waves. These waves travel through the component and may be captured by sensors installed on the component's surface.

This technique is currently applied on isolated components.

In the nuclear industry, the AE technique is particularly applied for detecting leaks.

During the load test, the reactor internals were in place, the thimbles pulled back, and without any fuel elements in the RPV. In addition, the primary system was operating in solid mode (water liquid phase).The steam generators were filled with water and under a nitrogen blanket (target secondary pressure was between 66 and 68 bar abs). The reactor coolant was heated up to about 140 °C through the reactor coolant pumps and the pressure was increased through the charging pump of the Chemical and Volumetric Control System (CVCS). During the acoustic emission (AE) measurements the reactor coolant pumps were inactive, while the CVCS charging pumps remained in operation to maintain the pressure.

The load test was performed above 175 bar abs. For reference, normal operating pressure is 155.1 bar abs and the RPV design pressure is 172.3 bar abs. Prior to the test, a verification of the acceptability of the test conditions was carried out for all connected components.

The primary pressure evolution during the load test was in accordance with the Electrabel procedure and AE requirements and is given in Figure 6.1. There were two test plateaus at about 177 bar abs of respectively one hour and 30 minutes separated by a lower plateau at 158 bar abs. This enabled the detection of potential AE reactivation at a lower pressure level.

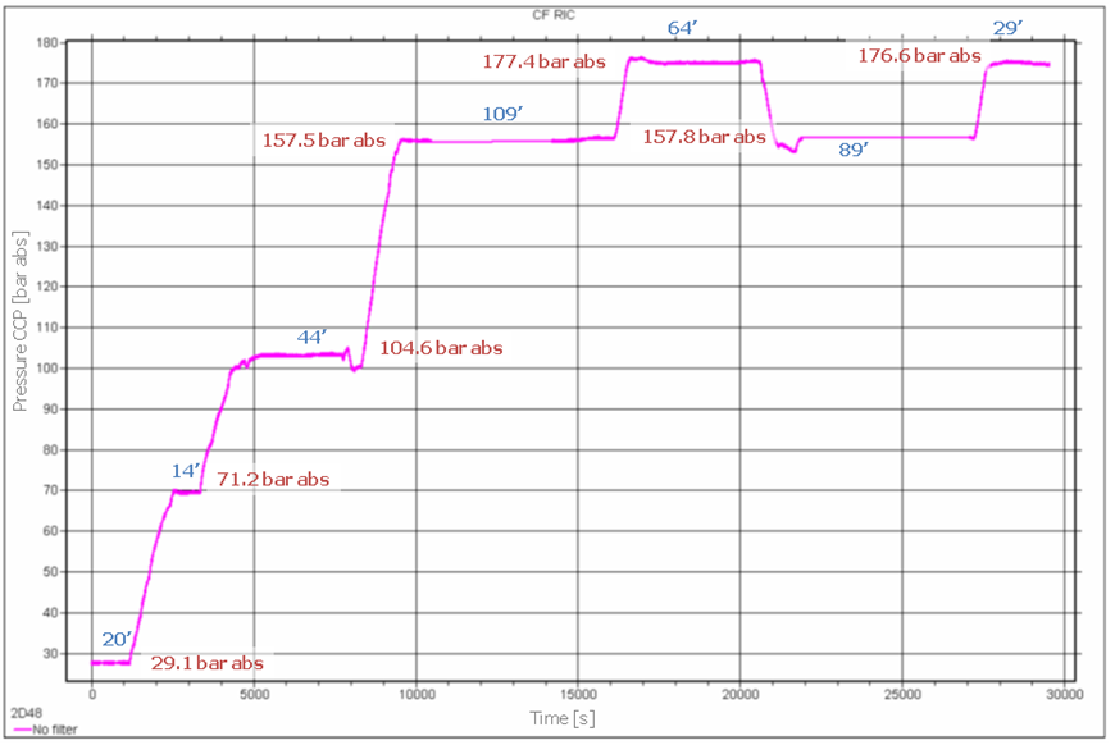


**Figure 6.1: Primary pressure evolution during the load test**

# 6.2 Acoustic Emission Test

The goal of the Acoustic Emission (AE) test was to detect the propagation of flaws in the RPV core shells, if any. In order to reach this objective, the Doel 3 RPV was equipped with fifteen sensors (see Figure 6.2):

- Six sensors on the Reactor Vessel Head.
- Six sensors on the RPV inlet and outlet nozzles.
- Three sensors on the in-core instrumentation connected to the bottom of the RPV.

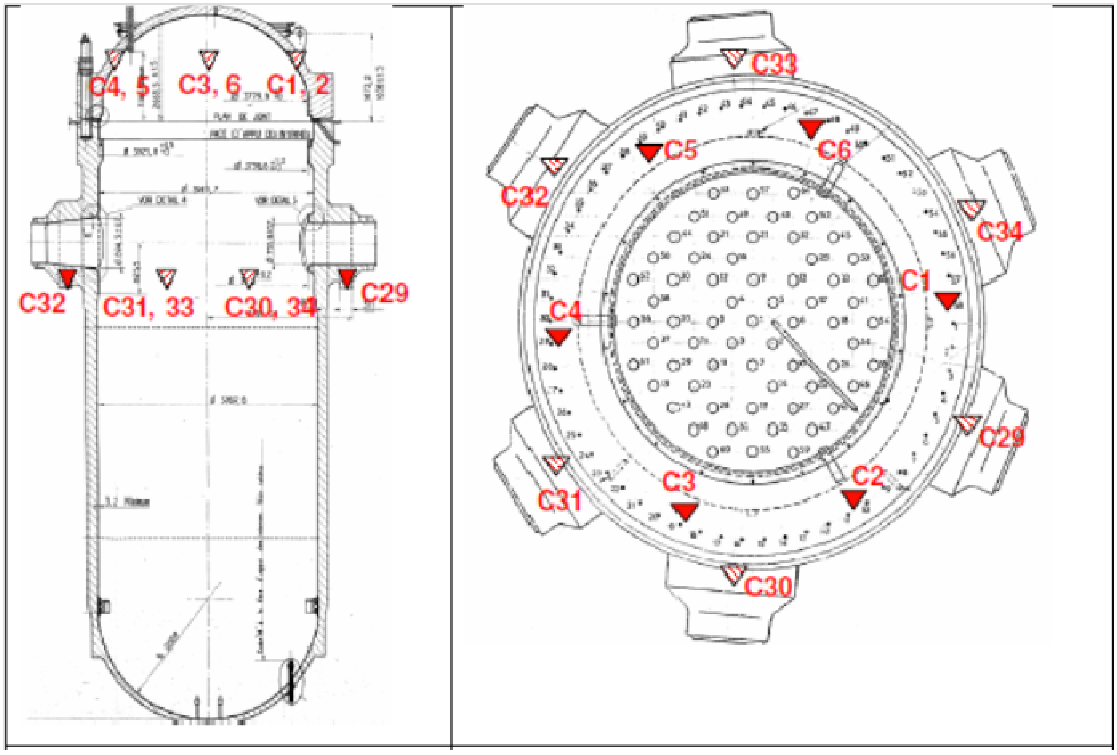


**Figure 6.2: Location of the sensors on the RVH (C1 to C6 and on the RPV nozzles (C29 to C34)**

This distribution of sensors enables the determination of AE sources (such as propagating flaws) in a specific 60° sector of the RPV. Based on a number of criteria, the AE sources and the areas where they are located are classified into three categories according to the Association Française des Ingénieurs en Appareils à Pression (AFIAP) best practices guideline for AE inspection of pressure vessels:

- Category I: Non-significant sources and/or areas.
- Category II: Sources and/or areas for which supplementary investigations are recommended.
- Category III: Critical sources and /or areas for which supplementary investigations are mandatory.

### Conclusions

The AE measurements performed on the Doel 3 RPV did not reveal any Category III AE source or area. No complementary investigations have to be conducted.

Since the AE measurements were performed on the RPV as part of the pressurized primary system and not on the RPV as an isolated equipment (as assumed in the AFIAP guidelines), there was an intensive acoustic activity related to operating events. Therefore, it was impossible to distinguish events related to operating conditions from events potentially happening at the material level. As a consequence, all AE sources and/or areas were classified in Category II. Further analysis of the AE measurements showed that the majority of acoustic emission activity took place before reaching the normal operating pressure. Based on the remaining Category II events, complementary UT investigations in one 60° angular sector of the RPV core shells were recommended. The area of the lower core shell with the highest density of indications detected during the 2012 UT inspection is located in this sector.

## 6.3 Post-Load Test UT Inspection

The goal of the post-load test inspection of the Doel 3 RPV was to detect any possible evolution of the material condition or flaws caused by the load test. The inspection was performed on the complete lower and upper core shell of the Doel 3 RPV. This covers the sector mentioned above. The inspection was executed in exactly the same way as the 2012 RPV inspection, using the same inspection tool, methods and settings.

The conclusion on evolution or non-evolution of the flaws between both inspections is based on quantitative criteria that consider the differences measured between successive examinations on the amplitude of the ultrasonic signals reflected by the flaw indications and on the ultrasonic measurements of the dimensions of the flaw indications.

### Conclusions

- The number of flaw indications reported by the post-load test inspection is fully consistent with the findings of the 2012 RPV inspection.
- The peak amplitude and dimensions of every indication reported by the post-load test inspection match those of the 2012 RPV inspection.

Therefore, it can be concluded that no evolution of the flaws was induced by the load test of the Doel 3 RPV.

# 7 List of Abbreviations

| | |
|---|---|
| **AE** | Acoustic Emission |
| **AFIAP** | Association Française des Ingénieurs en Appareils à Pression |
| **AIA** | Approved Inspection Authority |
| **ASME** | American Society for Mechanical Engineers |
| **CEA** | Commissariat à l'Energie Atomique et aux Energies Alternatives |
| **CVCS** | Chemical and Volumetric Control System |
| **DSR** | Défauts Sous Revêtement |
| **DTR** | Défauts Technologiques de Revêtement |
| **EAR** | Examen d'Accrochage du revêtement (specific straight beam transducer) |
| **Ev** | Label for individual flaw |
| **FANC** | (Belgian) Federal Agency for Nuclear Control |
| **FCG** | Fatigue Crack Growth |
| **FIS** | Formule d'Irradiation Supérieure |
| **FE** | Finite Element |
| **GP** | Label for grouped flaws |
| **LOCA** | Loss-Of-Coolant-Accident |
| **MIS-B** | Machine d'Inspection en Service Belge |
| **MT** | Magnetic Testing |
| **ppm** | Parts per million |
| **PTS** | Pressurized Thermal Shock |
| **RPV** | Reactor Pressure Vessel |
| **$RT_{NDT}$** | Reference Temperature for Nil Ductility Transition |
| **SCP** | Service de Contrôle Physique (Electrabel) |
| **SI** | Safety Injection |
| **SIA** | Structural Integrity Assessment |
| **SIF** | Stress Intensity Factor |
| **T** | Tilt |
| **UT** | Ultrasonic Testing |